Osteoarthritis and Cartilage 27 (2019) 1075–1083

Osteoarthritis and Cartilage

Clinical Trial

Proof of concept: hip joint damage occurs at the zone of femoroacetabular impingement (FAI) in an experimental FAI sheep model

C.A. Zurmühle †, F. Schmaranzer † *, K. Nuss ‡, N. Wolfer ‡, M.K. Ryan §, G. Zheng ‖, B. von Rechenberg ‡, M. Tannast † ‡ ¶

† *Department of Orthopaedic Surgery, Inselspital, Bern University Hospital, University of Bern, Bern, Switzerland*
‡ *Musculoskeletal Research Unit (MSRU), Equine Hospital, Vetsuisse Faculty, University of Zürich, Zürich, Switzerland*
§ *Andrews Sports Medicine and Orthopaedic Center, American Sports Medicine Institute, Birmingham, AL, USA*
‖ *Institute for Surgical Technology and Biomechanics, University of Bern, Bern, Switzerland*
¶ *Department of Orthopaedic Surgery and Traumatologie, Cantonal Hospital, University of Fribourg, Switzerland*

ARTICLE INFO

Article history:
Received 7 November 2018
Accepted 3 April 2019

Keywords:
Femoroacetabular impingement
Cam deformity
Osteoarthritis
Sheep hip model
Hip preservation surgery
CT impingement simulation

SUMMARY

Objective: In ovine hips chondrolabral damage as seen in cam-type femoroacetabular impingement (FAI) can be induced via an intertrochanteric varus osteotomy. However, it is yet to proven whether the observed cartilage damage is caused by a dynamic cam type impingement. Thus we asked, (1) whether actual cartilage damage observed after FAI induction in ovine hips occurs at the predicted, computed zone of FAI; (2) whether the extent of cartilage damage increases with ambulation time in this animal model?

Design: In this experimental, controlled, comparative study 20 sheep underwent unilateral FAI induction through an intertrochanteric varus osteotomy. Preoperatively sheep underwent computed tomography to generate three-dimensional models of the osseous pelvis and femur. The models were used to predict impingement zones before and after simulated varus osteotomy using range of motion (ROM) analysis. Sheep were sacrificed after 14–40 weeks of ambulation. At sacrifice cartilage was inspected and (1) location of actual damage and computed impingement zones were compared; (2) Cartilage damage was compared between short- and long ambulation groups.

Results: (1) The average location and the extent of peripheral and central cartilage lesions did not differ with the computed impingement zones (all $P > 0.05$). (2) Grades of central, posterior cartilage damage were more severe in the long-compared to the short ambulation group (2.2 ± 1.8 vs 0.4 ± 0.5; $P = 0.030$).

Conclusions: In this experimental ovine FAI model the surgical induction of an osseous impingement conflict between the femur and acetabulum causes cartilage damage at the zone of simulated FAI.

Introduction

Recently, a sheep model was introduced for experimental induction of cam-type femoroacetabular impingement (FAI)[1]. Such a model could be of vast scientific interest since it would offer a platform to investigate the natural course of FAI, the histological effect of cartilage therapies in this context, and the evaluation of novel biochemical imaging methods[2,3]. In this sheep model, the experimental FAI conflict is surgically induced by means of an extraarticular closed-wedge varus intertrochanteric osteotomy (Fig. 1). With this method, we demonstrated that focal degenerative lesions of the chondrolabral complex can be reliably provoked resembling those in young patients with FAI[1]. It has been suggested that this osteotomy places the naturally aspherical portion of the ovine femoral head closer to the acetabulum, thereby creating a dynamic inclusion-type pathomechanism as seen in cam-FAI which occurs at the limits of the range of motion (Fig. 1)[1].

However, despite this 'dynamic' explanation for the observed joint damage, cartilage lesions could alternatively result from

* Address correspondence and reprint requests to: F. Schmaranzer, Department of Orthopaedic Surgery Inselspital, Freiburgstrasse CH, 3010, Bern. Tel: 41-31-632-2222; Fax: 41-31-632-3600.
E-mail address: florian.schmaranzer@insel.ch (F. Schmaranzer).

https://doi.org/10.1016/j.joca.2019.04.001
1063-4584/

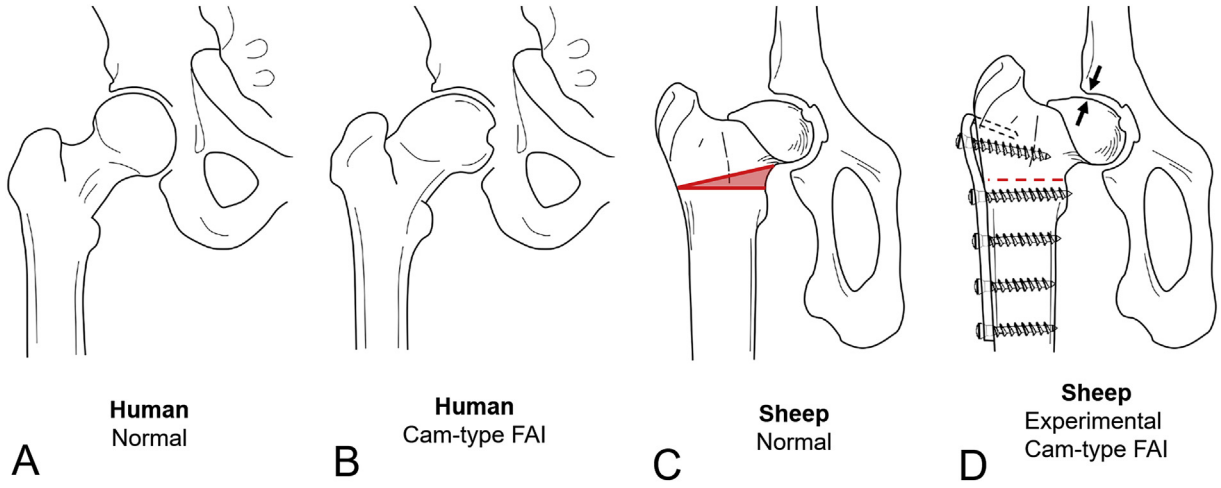

Fig. 1. This figure shows schematically (A) a normal configuration and (B) a cam-type deformity of the proximal femur in human beings. The sheep hip has a naturally present aspherical portion (C), which leads to an induced inclusion-type femoroacetabular impingement (FAI) by performing a closed wedge intertrochanteric varus osteotomy.

changes of 'static' hip joint forces, as proven for intertrochanteric varus[4,5] or femoral shortening osteotomies[6] in human beings. As opposed to an impingement conflict which is triggered at specific, high arcs of motion, an increase in static hip joint forces would occur during any weight bearing activity of the hip including standing and normal gait[7]. In addition, such an intertrochanteric osteotomy can potentially alter the blood supply to the epiphysis leading to avascular necrosis and thereby affecting the joint cartilage. Although the inferential evidence of this experimental FAI model we have provided so far suggests that chondrolabral lesions are caused by the 'dynamic' FAI conflict[1], the concurrence of the actual impingement zones and resulting joint damage has yet to be confirmed. In human beings, this cause-and-effect relationship between macroscopic joint damage and location of impingement has already been established with modern CT-based virtual impingement simulation[8].

The aim of this study was to establish a similar causation for the experimental ovine FAI model thereby establishing the proof of concept of this promising FAI model. Therefore we asked, (1) whether actual cartilage damage observed after FAI induction in ovine hips occurs at the predicted, computed zone of FAI, and (2) whether the extent of cartilage damage increases with ambulation time in this animal model.

Methods

Experimental animals

This study was conducted according to Swiss laws for animal welfare. It was approved by the local governmental authorities (Kantonales Veterinäramt Zürich, Switzerland, No. 2/2014 and 099/2017). The experiments were performed in compliance with principles of Good Laboratory Practice of the World Health Organization[9]. We performed a prospective, experimental, comparative study on 20 female Swiss Alpine sheep (mean age of 1.9 ± 0.5 years [range, 1.2–2.8 years], mean weight of 60 ± 7 kg [range, 49–76 kg] and mean ambulation time of 26 ± 9 weeks [range, 14–40 weeks]) (supplementary table I). The number of sheep and the ambulation time was chosen similar to the initial description of this model in which the cam FAI like topographic- and macroscopic pattern of cartilage damage was established based on 16 sheep (ambulation time of 14–38 weeks) after FAI induction[1]. This easily available animal was selected due to its comparable hip anatomy with a horseshoe shaped acetabulum, the presence of an acetabular fossa and labrum, little inter-individual morphological variability[10] (supplementary table I), lack of predisposition for primary hip osteoarthritis[11], comparable contact pressure magnitudes/distribution[12], and mean surface stresses to human beings[13]. Furthermore sheep due to their relative insensitivity to pain maintain high activity levels after experimental hip surgeries[11]. Most importantly, sheep exhibit a natural aspherical femoral head comparable to patients with a cam-type deformity that is normally positioned beyond the range of impingement during ovine quadrupedal gait[1]. Twenty sheep (20 hips) underwent unilateral surgical induction of FAI via a standardized intertrochanteric, varus osteotomy, which positions the aspheric portion of the head in a position creating cam-type impingement[1]. The contralateral side was used as a healthy control. We then compared the observed actual macroscopic joint damage after sacrifice with the preoperatively predicted computed tomography (CT)-based impingement zones.

Preoperative computed prediction of impingement zones

Preoperatively, all 20 sheep underwent a CT scan with 1.5 mm slice thickness (Somatom Sensation Open, Siemens Medical Solutions, Erlangen, Germany) which included the entire pelvis and femur with the femoral condyles (voltage 120 kVp; intensity 300 mAs; pitch 0.65; field of view 50 cm; voxel size 1 mm^3, reconstruction kernels B20 and B60). For computer-based range of motion (ROM) analysis, we used a specifically designed and validated software 'HipMotion' (University of Bern, Switzerland)[14,15]. The CT scan was used for semi-automatic segmentation of 3D models of the osseous pelvis and femur using commercially available software (Amira 5.4, Visage Imaging Inc., Carlsbad, CA, USA). The generated 3D models of the pelvis and femur were used as input data for the motion analysis[16].

Analogous to human beings, the calculation of ROM and the location of the impingement zones were computed based on the following reference coordinate systems (Fig. 2)[17]. For the pelvis, both anterosuperior iliac spines (ASIS) and the pubic tubercles created the anterior pelvic reference plane (APP). For the femur, rotation centers of the hip and knee created the femur axis with the posterior aspects of the femoral condyles as reference for rotation[14]. Due to the quadrupedal gait in sheep, and in contrast to human beings, a neutral hip flexion is defined with the femoral axis perpendicular to the APP (Fig. 2)[1]. Using these references, the

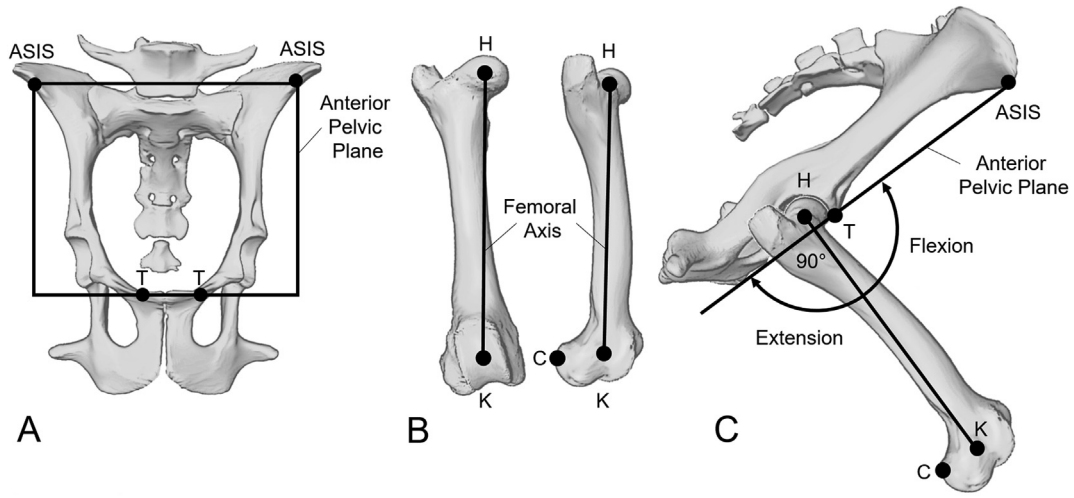

Fig. 2. The reference coordinate systems for the three-dimensional motion simulation are shown for the pelvis (A) and the femur (B). The pelvic reference coordinate system is the anterior pelvic plane, which is defined by both anterior superior iliac spines (ASIS) and the pubic tubercles (T). The femoral axis is defined by the hip (H) and knee (K) center with the femoral condyles (C) as reference for rotation. (C) Due to the quadrupedal gait of sheep, the neutral zero position was defined with the femur axis being perpendicular to the anterior pelvic plane.

physiological posture of a standing sheep corresponds approximately to 20° of flexion, 20° of external rotation, and 5° of abduction (supplementary Fig. 1)[18]. Based on the segmented 3D pelvic models, we created digitally reconstructed radiographs (DRR) of the pelvis with the APP in neutral position for further descriptive coxometric analysis of the anatomy. All DRRs were then analyzed using a previously validated software (Hip[2]Norm, University of Bern, Bern, Switzerland; supplementary table I)[19–21]. Femoral version was measured according to the method of Murphy (supplementary table I)[22].

Software HipMotion (University of Bern, Bern, Switzerland) includes fully-automatic algorithms for identification of the acetabular rim[23] and the definition of the femoral head center based on a best fitting-sphere[24]. Most specifically for this software and in particular useful in non-spherical hips as seen in sheep, the software uses a specific motion algorithm called the 'equidistant' method[25]. This method calculates ROM based on incremental 1° increase of motion and detects surface contact areas between the femur and the acetabulum. Using these surfaces, two best fitting spheres were calculated (one for the femoral head and one for the acetabulum), of which both centers of rotation were matched for every motion[24]. This method reduces errors resulting from joint irregularities and enables the 3D virtual joint motion in largely deformed and non-contained hips (e.g., Legg-Calvé-Perthes disease)[26]. It is therefore best suitable for the hip motion analysis in sheep. A previous validation study of HipMotion showed an accuracy of 2.6° ± 2.5° for hip motion and 1.3 mm ± 1.2 mm for detection of the impingement zones with high interobserver reproducibility (intraclass correlation coefficient [ICC]: 0.88–0.99) and intraobserver reliability (ICC: 0.87–0.95)[14].

ROM was studied in 5° increments between flexion/extension 60-0-90°, internal/external rotation 0-10-30°. This arc of hip flexion/extension was chosen in accordance to previously published goniometric measurements of the hindlimb in sheep and illustrations of a gait cycle in sheep (supplementary Fig. 1)[18,27]. The arc of hip rotation was based on preoperative goniometric measurements of the hindlimb of ten sheep under anesthesia (mean internal rotation/external rotation, 0-10-25°). Similarly, the physiologic abduction/adduction arc was determined 20-0-10°in sheep. These parameters were used to calculate the normal values for the gait cycle in sheep (supplementary table I). For the simulation of a 15° varus osteotomy[1] we added 15° to the arc of abduction-adduction accordingly which eventually resulted in an amplitude of 35-5-0°.

We then quantified the individual impingement points for each possible combination of motion. We performed a cluster analysis in order to reduce the number of incidental impingement locations related to stair-step artifacts of the CT scan. Ward's method for hierarchical cluster analysis was applied for flexion/extension, abduction/adduction, internal/external rotation, and the number of impingement points[28]. This left an average of 1987 impingement points in 571 different, simulated hip motion steps per sheep. Presence of intra-articular and extra-articular impingement zones was recorded. Similar to the topographic analysis of human beings, the intraarticular impingement zones were categorized according to twelve sectors based on the clock face with 6 o'clock located in the acetabular notch (Fig. 3). The intraarticular impingement zones were further subdivided into a peripheral and central regions[8] (Fig. 3).

Experimentally induced impingement zones

Preoperative management and anesthesia was performed according to the previously published institutional standard protocol for surgery in sheep. Anesthesia was induced through a jugular catheter. An intravenous constant-rate infusion of propofol plus a maximum 5% isoflurane (Minrad Inc., Buffalo, NY, USA) inhalation was used for maintenance. Preoperative antibiotic prophylaxis included intravenous penicillin (35,000 IU/kg, Streuli Pharma, Uznach, Switzerland) and gentamycin (4 mg/kg, Vetagent, MSD Animal Health Care, Lucerne, Switzerland) for 4 days. Furthermore, we administered a subcutaneous injection of tetanus serum (3 ml, MSD Animal Health Care, Lucerne, Switzerland). The postoperative pain management included epidural anesthesia (0.01 mg/kg Morphin-HCL, Sintetica S.A., Mendrisio, Switzerland) and analgesics peri-/postoperatively (2–5×/per day intramuscular buprenorphin [0.01 mg/kg Temgesic, Essex Chemie AG, Luzern, Switzerland], 2×/per day intravenous paracetamol [1 ml/kg, Fresenius Kabi, Oberdorf, Switzerland) for 3 days. Neuromuscular blocking was performed with intravenous Rocuronium (0.06 mg/kg of 50 mg/ml Rocuronium Fresenius, Fresenius Kabi, Oberdorf, Switzerland). This was based on our experience with performing surgery in sheep. We

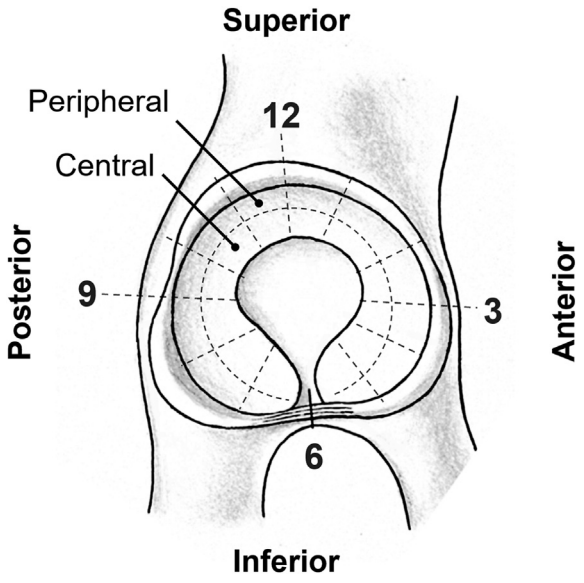

Fig. 3. This figure shows a schematic drawing of a right sheep hip to illustrate the clock face analysis for acetabular cartilage lesions. Six o'clock is defined at the acetabular notch. Each of the 12 sectors was further subdivided into a central and peripheral portion.

used a neuromuscular block following empiric testing for dose finding. Since no drainage of the wound was possible, electrocautery had to be used for surgical hemostasis. Without a neuromuscular block this would have led to almost uncontrollable muscle contractions in the sheep. Furthermore a neuromuscular block enables an easier and more controllable repositioning.

We used the same surgical technique as reported in the original description of surgical induction of FAI in sheep[1]. In brief, with the animal in lateral decubitus position, we performed a standard subvastus approach using a slightly curved incision centered over the greater trochanter. The femur is approached through the interval between the gluteobiceps muscle posteriorly and the vastus lateralis muscle anteriorly. A specifically designed cutting jig was then applied to the femur enabling a reproducible closed wedge varus osteotomy of 15°. Rotational alignment was controlled for with the linea aspera. Final reduction was performed manually. The osteotomy was then secured with a specifically developed 3.5 mm locking plate (Jossi Orthopedics, Islikon, Switzerland; supplementary Fig. 2).

Postoperatively, animals were kept in a suspension system for 4 weeks[1]. The suspension device was specifically designed to prevent the sheep from lying down and getting up. After 4 weeks, sheep were kept in small three-sheep pens for 2 weeks and were permitted to roam freely after a total of 6 weeks postoperatively. During spring and summer they were kept on the side of a mountain, where they could roam freely in an extensive, fenced area. During fall and winter sheep were kept in large paddocks which allowed them to roam. The ambulation time was set according to predetermined intervals of 2–3 weeks. This was done based on our earlier experience using an ambulation time of 14–38 weeks to ensure a representative extent of the cartilage damage[1]. Mostly due to logistic reasons no randomization was performed since this study was performed at an academic veterinary hospital which had to maintain its usual workflow during the study period and the available infrastructure had to be shared. Therefore only 2–4 animals entered a study cycle at a time. For statistical analysis all sheep were then allocated to two groups: the short ambulation group consisting of 10 sheep with an ambulation time of less than 25 weeks (mean 18 weeks; range, 14–22 weeks), and a long ambulation group consisting of 10 sheep with an ambulation time of more than 25 weeks (mean 34 weeks; range, 27–40 weeks). The two ambulation groups did not differ in terms of age, weight and radiographic anatomy (supplementary table II). After the predetermined ambulation time, sheep were euthanized via an intravenous injection of 30–40 ml Pentobarbital (300 mg/ml; Esconarkon, Streuli Pharma AG, Uznach, Switzerland). After sacrifice, all hips (the operated and the contralateral, healthy controls) were disarticulated and macroscopic acetabular cartilage lesions were documented dichotomously as either present or absent by two readers with extensive experience in clinical and experimental FAI surgery (KN, MT) in consensus. At the time of analysis both readers were blinded to the duration of the assigned ambulation time of the sheep and to the joint site (surgical FAI induction or control). Localization and extent of acetabular cartilage lesions was recorded analogously using the clock-face system and served as gold standard for comparison with simulated impingement locations from the computer analysis[8] (Fig. 3).

Analysis

We used the Kolmogorov–Smirnov test to assess normal distribution. Since not all study variables were normally distributed, only non-parametric tests were applied using SPSS 21.0 (IBM, Chicago, IL, USA). Descriptive statistics were calculated including 95% confidence intervals. For research question 1, we used the Mann–Whitney *U* test to compare the median impingement clock face positions between the sum of distributions of the actual and the computed impingement zones. The topographic extent (variance) between the actual and computed impingement zones was compared using Levene's test. In order to do that the dichotomous parameters of clock face zones with simulated and actual impingement zones were transformed from a relative distribution into equivalent continuous data analogously to a previously published approach[8]. For research question 2, we compared the mean prevalence and cartilage grades using the Beck *et al.*[30] classification of peripheral/central, anterior/posterior cartilage lesions between the short and the long ambulation group using the Mann–Whitney *U* test. Furthermore we described the variability for actual cartilage lesions as graded with the Beck *et al.*[30] classification (supplementary table III). This classification grades cartilage lesions into normal, malacia, debonding, cleavage and defect (grades 0–4)[30]. All *P*-values are two tailed and a $P < 0.05$ indicated statistical significance.

Results

The average location of the actual peripheral acetabular cartilage lesions (median 9 o'clock, twenty fifth percentile 8 o'clock/seventy fifth percentile 10 o'clock, range 1–12 o'clock) did not differ from the computed impingement zones (9 o'clock, 8/10 o'clock, range 1–12 o'clock, $P = 0.373$, Fig. 4(A)). The location of the actual central acetabular cartilage lesions (4 o'clock, 3/8 o'clock, range 1–12 o'clock) did not differ to the computed impingement zones (4 o'clock, 2/5 o'clock, range 1–12 o'clock, $P = 0.301$, Fig. 4(B)). There was no difference between the extent of the actual and computed peripheral impingement zones (variance 3.3 h vs 3.3 h, $P = 0.972$). There was no difference between the extent of the actual and computed central impingement zones (variance 12.7 h vs 11.5 h, $P = 0.186$). All impingement zones were intraarticular, there were no extraarticular impingement zones. The impingement conflict typically occurred with increasing extension, abduction, and with any rotation deviating from the physiological external rotation of 20° (Fig. 5, supplementary Fig. 3). At macroscopic inspection after

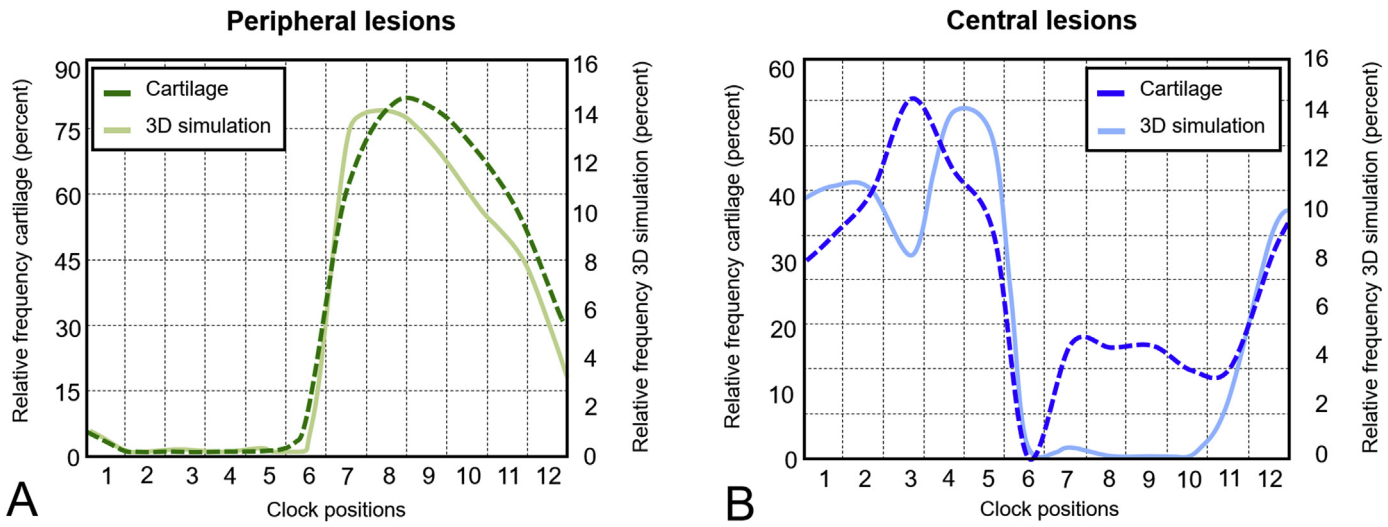

Fig. 4. The lines represent the relative distribution of the actual and simulated cartilage damage for each of the 12 'full-hour' positions of the clock face. (A) The actual cartilage damage in the peripheral acetabulum produced by the experimental FAI induction did not differ significantly both for median and variance with the simulated impingement zones. (B) Similarly, there was no difference between the actual central cartilage damage in the experimental setup compared to the simulated impingement zones both for the median and the variance.

sacrifice none of the contralateral control hips had acetabular cartilage lesions.

No difference between the mean prevalence of peripheral and central cartilage lesions was detected between the short- and the long ambulation group (Table I). Mean grades for severity of posterior centrally located cartilage lesions were higher for the long ambulation group compared to the short ambulation group (2.2 ± 1.8 vs 0.4 ± 0.5; mean difference 1.8 ± 1.7 [95% confidence interval 0.6–3; $P = 0.030$]) (Table I).

Discussion

In human beings, the association between a cam-type morphology, the resulting inclusion-type FAI pathomechanism and the observed chondrolabral damage is generally accepted[7]. This is based on the concurrence of the computed impingement locations in 3D simulations[15,31], the cartilage degeneration on MRI[32–34], the intraoperative cartilage damage[30,35], altered joint contact stresses based on finite element analysis, and longitudinal, epidemiologic data[36]. However, all of these studies simultaneously fail to provide a definite satisfactory explanation for the cause of articular damage. The ultimate proof of such a causation has been shown by the correlation between computed impingement zones using dynamic CT based simulation and macroscopic joint damage in humans[8]. Analogously, we applied the same methodology in an experimental ovine FAI model to establish the proof of concept of this translational approach.

This study has limitations. First, the actual ROM relative to anatomical reference coordinate systems is not exactly known in sheep, which is difficult to assess clinically in a standardized fashion. We established a dedicated ROM protocol based on previously reported goniometric measurements in unanesthetized sheep and our clinical experience with examination under sedation and observations of the osteological collection from our institution. Our flexion/extension range is larger than the reported arc based on goniometric measurements in healthy sheep (supplementary table I). This can be explained with the second limitation, namely the fact that CT-based impingement simulation is based on osseous models

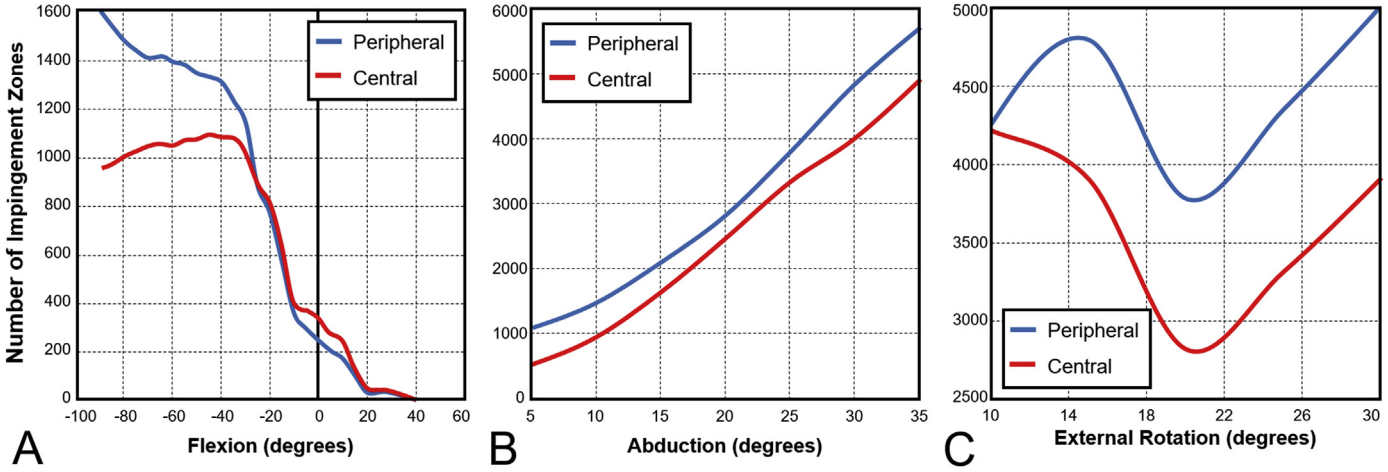

Fig. 5. The lines represent the number of impingement zones for each simulated degree of the range of motion (ROM) simulation. The number of impingement zones increases with (A) hip extension, (B) abduction, and (C) any rotational deviation starting from the physiological external rotation of 20°.

Table I
Prevalence and grading of severity of cartilage damage for the ambulation groups

Parameter	Short ambulation group	Long ambulation group	Mean difference
Mean prevalence of zones with peripheral cartilage damage, (%)			
Anterior	0 ± 0	3 ± 7	3 ± 7 (−2 − 8); $P = 0.146$
Posterior	62 ± 25	63 ± 25	2 ± 43 (−29 − 33); $P = 0.908$
Mean prevalence of zones with central cartilage damage, (%)			
Anterior	50 ± 14	52 ± 24	2 ± 21 (−14 − 17); $P = 0.578$
Posterior	18 ± 33	35 ± 39	17 ± 52 (−20 − 54); $P = 0.200$
Mean Beck *et al.*[30] grading (grade 0 − grade 4) for peripheral cartilage damage			
Anterior	0 ± 0	0.4 ± 1	0.4 ± 1 (−0.3 − 1.1); $P = 0.147$
Posterior	1.7 ± 0.8	2.3 ± 0.8	0.5 ± 1.4 (−0.4 − 1.5); $P = 0.185$
Mean Beck *et al.*[30] grading (grade 0 − grade 4) for central cartilage damage			
Anterior	1.6 ± 1.3	2.3 ± 1.6	0.7 ± 2.6 (−1.1 − 2.5); $P = 0.385$
Posterior	0.4 ± 0.5	2.2 ± 1.8	**1.8 ± 1.7 (0.6 − 3); $P = 0.030$**

Values are expressed as mean and standard deviation with 95% confidence intervals in parentheses. Bold numbers refer to a significant difference (p<0.05).

of the pelvis and femur only. It does not consider the labrum, cartilage, joint capsule, and the surrounding soft tissues. While the calculation of the impingement zones remains accurate, this leads to an overestimation of the natural ROM explaining our findings[14,25]. Third, we did not use a postoperative CT scan for 3D analysis. Instead, we deliberately used the preoperative CT scan with a virtual FAI induction to prevent segmentation errors resulting from metal artifact related to the plate, which would have negatively affected the accuracy of the impingement simulation. Fourth, we used a dichotomous grading of macroscopic joint damage without a more detailed description to answer the first research question. This was done to facilitate the statistical analysis which would have been further complicated by a semiqualitative grading. However analogously to previous studies using this model we added a more detailed semiqualitative analysis of cartilage damage pattern to assess whether severity of damage increases with ambulation time (Table I) and to illustrate the variability for actual lesions (supplementary table III)[1,30]. Fifth, a systematic histologic analysis of cartilage damage was not included in this study. However in a clinical setting the intraoperative inspection of the macroscopic cartilage damage is still the diagnostic gold standard as it guides intra-operative decision making and is the most important prognostic factor for success of joint preserving surgery of the hip[8,37]. Furthermore it was our intention to use this translational animal model under the same conditions as the initial study in human FAI in which the causal relationship between zones

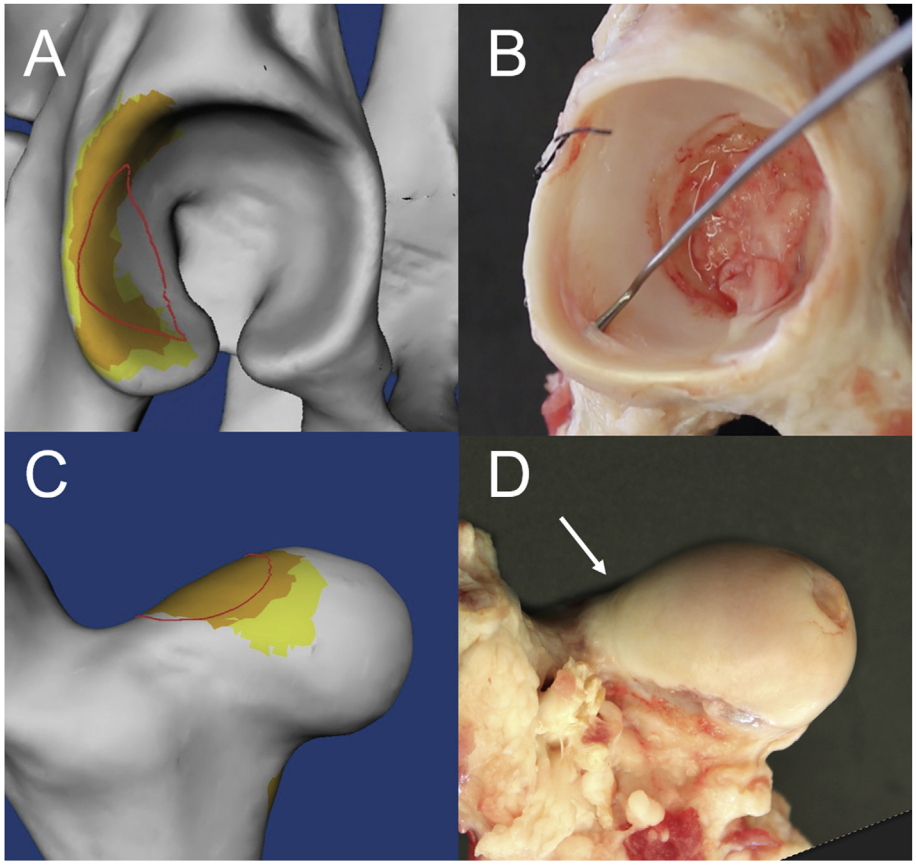

Fig. 6. (A) Three-dimensional analysis with impingement zones located between 7 and 10 o'clock. (B) Correspondingly, the chondrolabral lesions are located in the same area. (C) The simulated impingement area of the femoral head is located at the aspherical portion. (D) A saddle-back deformity forms over time at this location.

of impingement and actual macroscopic cartilage damage has been established[8]. Apart from that the histologic pattern of cartilage damage has been previously reported several times for this animal model (supplementary Fig. 4)[1–3].

We demonstrated that the experimentally induced cartilage damage in sheep corresponds to the simulated impingement locations. Interestingly and in contrast to previous assumptions[1], the impingement conflict after FAI induction occurs predominantly in extension and not in flexion [Fig. 5(A)]. Consistent with other reports using this FAI sheep model, the majority of the observed peripheral acetabular cartilage lesions is confined to the posteroinferior acetabulum (peak at 9 o'clock, Figs. 4(A) and 6)[1,2]. This location is rotated 90° to that of human beings (anterosuperior) due to the quadrupedal nature of sheep. The majority of observed central acetabular lesions in our model was located anteroinferiorly (peak at 4 o'clock) - just opposite to the peripheral impingement zones (Fig. 4). One explanation would be the inherent loss of femoral version after varus osteotomy[38], which is equivalent to more external rotation in our model. This in turn can predispose to central impingement locations as shown by our simulation (Figs. 5(C) and 7). Another explanation for this consistent damage pattern is a posteroinferior inclusion type impingement in hip extension due to the aspherical femoral head with a contre-coup like lesion in the anterior central portion. A similar, but spatially inverted pathomechanism has been proposed in human beings: anterior impingement and posterior contre-coup through a levering-out mechanism[7]. By contrast, alternative explanations for the observed cartilage damage which could be explained by static or biological concepts are not plausible. Changing femoral alignment by 15° of varus reportedly results in a static increase of cartilage surface stress[5]. However, due to the spatial orientation of the pelvis in sheep, this should occur in the superior acetabulum and not posteroinferiorly as observed in our study. Similarly, an interruption of the femoral head blood supply after intertrochanteric osteotomy is unlikely, since it could be shown that the experimental FAI induction in sheep can be performed safely without the risk of avascular necrosis[29]. We interpret these results as proof that the peripheral chondral damage in the ovine FAI model is caused by inclusion type FAI with an opposed central contre-coup mechanism in hip extension.

While there was no time-dependent difference in extent and severity of peripheral cartilage lesions, we found an increased severity of central, posterior cartilage lesions over time. This can be explained by gradual deterioration of the cartilage lesions starting from the chondrolabral junction and further progressing centrally towards the acetabular fossa. In human beings, the degenerative cascade starts with a chondrolabral separation, a peripheral delamination of cartilage flaps, complete loss of cartilage integrity, subluxation of the femoral head into the defect, and eventually progression of the cartilage lesion towards the fossa[7,30]. The pattern and progression of these findings support the translational validity of this animal model for reproducible surgical FAI induction.

In summary, this study provides the proof of concept of a sheep FAI model due to the ability to perform same specimen controls, longitudinally follow and control the duration of exposure to the desired stimulus, and to correlate osseous impingement with

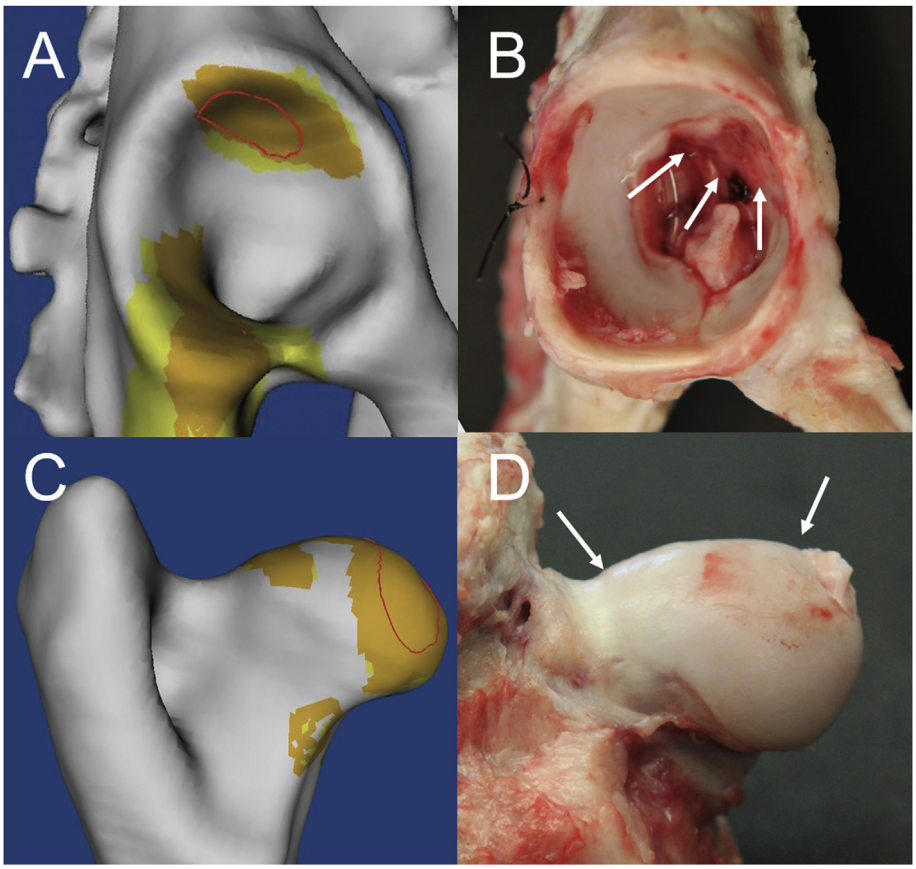

Fig. 7. (A) With a slight additional external rotation, a central impingement zone can be created between 12 and 2 o'clock. (B) The corresponding macroscopic lesion is present anterosuperiorly in addition to the posteroinferior chondrolabral lesion. (C) The central impingement is caused by a portion of the spherical femoral head. (D) The corresponding lesion is shown macroscopically in addition to the saddleback deformity.

macroscopic anatomical findings at the locations of interest within the joint. The induced cam FAI mechanism occurs mainly in extension and primarily causes posteroinferior, peripheral acetabular cartilage damage with secondary lesions in the anterosuperior acetabulum. Over time posteroinferior macroscopic damage progresses from the periphery towards the central joint cavity. These results confirm the pathomechanic role of surgically-induced cam-type impingement by means of a varus intertrochanteric osteotomy in the onset of damage to the hip joint and paves the way to further studies using this ovine FAI model.

Author contributions

CAZ: technical support for data acquisition, image data collection, analysis and interpretation of data, statistical analysis, initial draft, manuscript editing, final approval of the version to be submitted, ensures the integrity of the work.

FS: administrative, technical and logistic support for data acquisition, collection and assembly of data, statistical analysis, initial draft, final approval of the version to be submitted.

KN: administrative, technical and logistic support for data acquisition, collection and assembly of data, manuscript editing, final approval of the version to be submitted.

NW: administrative, technical and logistic support for data acquisition, collection and assembly of data, initial draft, final approval of the version to be submitted.

MKR: initial draft, manuscript editing, final approval of the version to be submitted.

GZ: technical support for computer simulation, manuscript editing, final approval of the version to be submitted, ensures the integrity of the work.

BvR: administrative, technical and logistic support for data acquisition, manuscript editing, final approval of the version to be submitted, ensures the integrity of the work.

MT: concept and design of the study, manuscript editing, final approval of the version to be submitted, ensures the integrity of the work.

Conflict of interest

No author has a commercial association that might pose a conflict of interest in connection with the submitted article.

Role of the funding source

This study was funded by the Swiss National Science Foundation (Project No. 144856). The funding sources had no role in study design, data collection, analysis, interpretation, writing or submission of the manuscript.

Supplementary data

Supplementary data to this article can be found online at https://doi.org/10.1016/j.joca.2019.04.001.

References

1. Siebenrock K, Fiechter R, Tannast M, Mamisch T, von Rechenberg B. Experimentally induced cam impingement in the sheep hip. J Orthop Res 2013;31(4):580–7, https://doi.org/10.1002/jor.22273.
2. Siebenrock K, Kienle K, Steppacher S, Tannast M, Mamisch T, von Rechenberg B. Biochemical MRI predicts hip osteoarthritis in an experimental ovine femoroacetabular impingement model. Clin Orthop Relat Res 2015;473(4):1318–24, https://doi.org/10.1007/s11999-014-3849-6.
3. Schmaranzer F, Arendt L, Liechti EF, Nuss K, von Rechenberg B, Kircher PR, *et al*. Do dGEMRIC and T2 imaging correlate with histologic cartilage degeneration in an experimental ovine FAI model? Clin Orthop Relat Res November 2018, https://doi.org/10.1097/CORR.0000000000000593.
4. Návrat T, Vrbka M, Florian Z, Rozkydal Z. Strain-stress analysis of pathological hip joint after osteotomy. Eng Mech 2008;15(5):345–54.
5. Schmitt J, Meiforth J, Lengsfeld M. Development of a hybrid finite element model for individual simulation of intertrochanteric osteotomies. Med Eng Phys 2001;23(8):529–39.
6. Wretenberg P, Hugo A, Broström E. Hip joint load in relation to leg length discrepancy. Med Devices (Auckl) 2008;1:13–8.
7. Ganz R, Leunig M, Leunig-Ganz K, Harris WH. The etiology of osteoarthritis of the hip: an integrated mechanical concept. Clin Orthop Relat Res 2008;466(2):264–72, https://doi.org/10.1007/s11999-007-0060-z.
8. Tannast M, Goricki D, Beck M, Murphy SB, Siebenrock KA. Hip damage occurs at the zone of femoroacetabular impingement. Clin Orthop Relat Res 2008;466(2):273–80, https://doi.org/10.1007/s11999-007-0061-y.
9. Becker RA, Janus ER, White RD, Kruszewski FH, Brackett RE. Good laboratory practices and safety assessments. Environ Health Perspect 2009;117(11):A482–3, https://doi.org/10.1289/ehp.0900884. author reply A483-484.
10. Maquer G, Bürki A, Nuss K, Zysset PK, Tannast M. Head-neck osteoplasty has minor effect on the strength of an ovine cam-FAI model: *in vitro* and finite element analyses. Clin Orthop Relat Res 2016;474(12):2633–40, https://doi.org/10.1007/s11999-016-5024-8.
11. Phillips TW, Johnston G, Wood P. Selection of an animal model for resurfacing hip arthroplasty. J Arthroplast 1987;2(2):111–7.
12. Mazoochian F, Hölzer A, Jalali J, Schmidutz F, Schröder C, Woiczinski M, *et al*. Finite element analysis of the ovine hip: development, results and comparison with the human hip. Vet Comp Orthop Traumatol 2012;25(4):301–6, https://doi.org/10.3415/VCOT-11-09-0132.
13. Bergmann G, Graichen F, Rohlmann A. Hip joint forces in sheep. J Biomech 1999;32(8):769–77.
14. Tannast M, Kubiak-Langer M, Langlotz F, Puls M, Murphy SB, Siebenrock KA. Noninvasive three-dimensional assessment of femoroacetabular impingement. J Orthop Res 2007;25(1):122–31, https://doi.org/10.1002/jor.20309.
15. Kubiak-Langer M, Tannast M, Murphy SB, Siebenrock KA, Langlotz F. Range of motion in anterior femoroacetabular impingement. Clin Orthop Relat Res 2007;458:117–24, https://doi.org/10.1097/BLO.0b013e318031c595.
16. Steppacher SD, Zurmühle CA, Puls M, Siebenrock KA, Millis MB, Kim YJ, *et al*. Periacetabular osteotomy restores the typically excessive range of motion in dysplastic hips with a spherical head. Clin Orthop Relat Res 2015;473(4):1404–16, https://doi.org/10.1007/s11999-014-4089-5.
17. Tannast M, Röthlisberger M, Gathmann S, Steppacher SD, Murphpy SB, Langlotz F, *et al*. In: Davies B, Joskowicz L, Leung K, Eds. The interrelationship among different reference coordinate systems systems of the pelvis- a computer assisted anatomical study. Berlin, Germany: Pro Business; 2008:185–8.
18. Govoni VM, Rahal SC, Agostinho FS, Conceição RT, Tsunemi MH, El-Warrak AO. Goniometric measurements of the forelimb and hindlimb joints in sheep. Vet Comp Orthop Traumatol 2012;25(4):297–300, https://doi.org/10.3415/VCOT-11-07-0098.
19. Tannast M, Mistry S, Steppacher SD, Reichenbach S, Langlotz F, Siebenrock KA, *et al*. Radiographic analysis of femoroacetabular impingement with Hip2Norm-reliable and

validated. J Orthop Res 2008;26(9):1199–205, https://doi.org/10.1002/jor.20653.
20. Zheng G, Tannast M, Anderegg C, Siebenrock KA, Langlotz F. Hip2Norm: an object-oriented cross-platform program for 3D analysis of hip joint morphology using 2D pelvic radiographs. Comput Methods Progr Biomed 2007;87(1):36–45, https://doi.org/10.1016/j.cmpb.2007.02.010.
21. Tannast M, Hanke MS, Zheng G, Steppacher SD, Siebenrock KA. What are the radiographic reference values for acetabular under- and overcoverage? Clin Orthop Relat Res 2015;473(4):1234–46, https://doi.org/10.1007/s11999-014-4038-3.
22. Murphy SB, Simon SR, Kijewski PK, Wilkinson RH, Griscom NT. Femoral anteversion. J Bone Joint Surg Am 1987;69(8):1169–76.
23. Puls M, Ecker TM, Steppacher SD, Tannast M, Siebenrock KA, Kowal JH. Automated detection of the osseous acetabular rim using three-dimensional models of the pelvis. Comput Biol Med 2011;41(5):285–91, https://doi.org/10.1016/j.compbiomed.2011.03.004.
24. Mahaisavariya B, Sitthiseripratip K, Tongdee T, Bohez ELJ, Vander Sloten J, Oris P. Morphological study of the proximal femur: a new method of geometrical assessment using 3-dimensional reverse engineering. Med Eng Phys 2002;24(9):617–22.
25. Puls M, Ecker TM, Tannast M, Steppacher SD, Siebenrock KA, Kowal JH. The Equidistant Method - a novel hip joint simulation algorithm for detection of femoroacetabular impingement. Comput Aided Surg 2010;15(4–6):75–82, https://doi.org/10.3109/10929088.2010.530076.
26. Tannast M, Hanke M, Ecker TM, Murphy SB, Albers CE, Puls M. LCPD: reduced range of motion resulting from extra- and intraarticular impingement. Clin Orthop Relat Res 2012;470(9):2431–40, https://doi.org/10.1007/s11999-012-2344-1.
27. Szunyoghy A, Ed. Anatomische Zeichenschule: Mensch, Tier. Köln: Könemann; 1996.
28. Ward J. Hierarchical grouping to optimize an objective function. J Am Stat Assoc 1963;58:236–44.
29. Schmaranzer F, Arendt L, Lerch TD, Steppacher SD, Nuss K, Wolfer N, *et al*. Femoral osteochondroplasty can be performed effectively without the risk of avascular necrosis or femoral neck fractures in an experimental ovine FAI model. Osteoarthrtis Cartilage 2018;26(1):128–37, https://doi.org/10.1016/j.joca.2017.10.009.
30. Beck M, Kalhor M, Leunig M, Ganz R. Hip morphology influences the pattern of damage to the acetabular cartilage: femoroacetabular impingement as a cause of early osteoarthritis of the hip. J Bone Joint Surg Br 2005;87(7):1012–8, https://doi.org/10.1302/0301-620X.87B7.15203.
31. Bouma HW, Hogervorst T, Audenaert E, Krekel P, van Kampen PM. Can combining femoral and acetabular morphology parameters improve the characterization of femoroacetabular impingement? Clin Orthop Relat Res 2015;473(4):1396–403, https://doi.org/10.1007/s11999-014-4037-4.
32. Schmaranzer F, Haefeli P, Hanke M, Liechti EF, Werlen SF, Siebenrock KA, *et al*. How does the dGEMRIC index change after surgical treatment for FAI? A prospective controlled study: preliminary results. Clin Orthop Relat Res 2017;475(4):1080–99, https://doi.org/10.1007/s11999-016-5098-3.
33. Hanke MS, Steppacher SD, Anwander H, Werlen S, Siebenrock KA, Tannast M. What MRI findings predict failure 10 Years after surgery for femoroacetabular impingement? Clin Orthop Relat Res 2017;475(4):1192–207, https://doi.org/10.1007/s11999-016-5040-8.
34. Schmaranzer F, Todorski IAS, Lerch TD, Schwab J, Cullmann-Bastian J, Tannast M. Intra-articular lesions: imaging and surgical correlation. Semin Muscoskel Radiol 2017;21(5):487–506, https://doi.org/10.1055/s-0037-1606133.
35. Ganz R, Parvizi J, Beck M, Leunig M, Nötzli H, Siebenrock K. Femoroacetabular impingement: a cause for osteoarthritis of the hip. Clin Orthop Relat Res 2003;417:112–20, https://doi.org/10.1097/01.blo.0000096804.78689.c2.
36. Agricola R, Heijboer MP, Bierma-Zeinstra SMA, Verhaar JAN, Weinans H, Waarsing JH. Cam impingement causes osteoarthritis of the hip: a nationwide prospective cohort study (CHECK). Ann Rheum Dis 2013;72(6):918–23, https://doi.org/10.1136/annrheumdis-2012-201643.
37. Ng VY, Arora N, Best TM, Pan X, Ellis TJ. Efficacy of surgery for femoroacetabular impingement: a systematic review. Am J Sports Med 2010;38(11):2337–45, https://doi.org/10.1177/0363546510365530.
38. Liu RW, Toogood P, Hart DE, Davy DT, Cooperman DR. The effect of varus and valgus osteotomies on femoral version. J Pediatr Orthop 2009;29(7):666–75, https://doi.org/10.1097/BPO.0b013e3181b769b5.